ECHINODERM SKELETAL PRESERVATION: CALCITE–ARAGONITE SEAS AND THE Mg/Ca RATIO OF PHANEROZOIC OCEANS

J.A.D. DICKSON
Department of Earth Sciences, University of Cambridge, Downing Street, Cambridge, CB2 3EQ, U.K.
email: jadd1@esc.cam.ac.uk

ABSTRACT: **The alternation between abiotic calcite and aragonite precipitation in shallow seawater and the oscillation of seawater Mg/Ca ratio throughout the Phanerozoic are both popular hypotheses. Echinoderms with well-preserved stereom provide new empirical evidence that supports both these hypotheses. Analyses are reported from 29 specimens, Cambrian to Eocene age, containing ossicles preserved either as Mg calcite, 3.3 to ~8 mole% $MgCO_3$, or as mixed calcite and dolomite, ~5 to 12.5 mole% $MgCO_3$. Echinoderms with high mole% $MgCO_3$ occur in the Early Cambrian and late Carboniferous to Triassic; low values come from the Silurian and Jurassic to Cretaceous. The average composition of echinoderms with preserved stereom does not fall below 3.5 mol% $MgCO_3$ during the Phanerozoic and reaches its highest mean value of 16.0 mol% $MgCO_3$ today.**

An empirical partition coefficient of 0.03182 for modern tropical echinoids is used to indicate the Mg/Ca ratio of ancient seawater from the Mg/Ca ratio of fossil stereom; some assumptions are involved and a likely error is calculated from the Mg^{2+} variation of modern echinoids. High mean seawater Mg/Ca ratios are calculated for early Cambrian (3.3) and the late Carboniferous to Triassic (2.3) but never reached today's value of 5.2; low Mg/Ca ratios (1.1) are indicated from Jurassic to Cretaceous echinoderms. The 29 echinoderm samples plot close to first-order Mg/Ca seawater oscillations derived from geochemical models and Mg/Ca ratios determined from fluid inclusions, but considerable discrepancies exist when shorter (10^6 Myr) time intervals are considered. Further data and improved understanding of Mg partitioning is required before accurate secular variation in the Mg/Ca of seawater can be determined from echinoderms. However, they are an underused resource in this context and provide an excellent seawater archive.

INTRODUCTION

Sandberg (1975) recorded a change from calcite to aragonite ooids during the Mesozoic that he related to changing Mg/Ca ratio of seawater; later (1983) he proposed that the dominant abiotic carbonate precipitated from shallow seawater oscillated between calcite and aragonite during the Phanerozoic Eon. He noted that this oscillation matched Fisher's (1981) icehouse–greenhouse cycles, which were, in turn, linked to changes in atmospheric PCO_2 (Mackenzie and Pigott 1981). Opinion has returned to seawater Mg/Ca ratio as the control on abiotic aragonite or calcite precipitation (Hardie 1996; Stanley and Hardie 1998, 1999; Stanley et al. 2002), although experimental work by Morse et al. (1997) indicates that temperature is equally important. Sandberg (1983) epitomized this mineralogical alternation as ''calcite and aragonite seas,'' terms that have been adopted by some, although their boundaries are ill-defined. Bates and Brand (1990) have criticized Sandberg's database and suggest that aragonite was the dominant abiotic carbonate to precipitate from Silurian to Recent seawater.

The notion that the concentration of major dissolved ions in seawater has remained constant during the Phanerozoic (Holland 1978) has been losing credence over the past two decades. Recent reviews strongly favor fluctuations in ocean chemistry throughout the Phanerozoic (Kerr 2002; Montañez 2002; Lemarchand 2003). This applies particularly to the Mg/Ca ratio, which is now predicted to have oscillated between 1 and 5 by geochemical modeling (Wilkinson and Algeo 1989; Hardie 1996) and fluid-inclusion studies (Lowenstein et al. 2001; Brennan and Lowenstein 2002; Horita et al. 2002). Marine carbonate precipitates should provide a direct means of monitoring Mg^{2+} and Ca^{2+} but are fraught with difficulties due to their susceptibility to diagenetic change and poor understanding of Mg partitioning (Morse and Bender 1990), especially with respect to biogenic carbonates (Zeebe and Sanyal 2002).

Fossil echinoderm skeletons have been ignored as potential marine proxies in the past because their stereom was thought to be always altered (Weber 1973). Echinoderm skeletal Mg calcite, however, can be altered along many different diagenetic pathways; some are preserved as Mg calcite and some undergo alteration to calcite and dolomite but with preservation of original bulk composition (Dickson 1995, 2001b, 2002). The use of fossil echinoderms in this context is explored further in this paper.

MATERIAL AND ANALYSIS

The preservation state of 104 samples of superficially well-preserved echinoderms was assessed using a Zeiss Axioplan petrological microscope and backscatter electron images from a Jeol 820 SEM (BSEM). Twenty-nine samples, some single ossicles and some rock samples containing many ossicles, were selected for this study (Table 1). All analyzed ossicles have well defined stereom microstructure; labyrinthic, galleried and rectilinear microstructural types (Smith 1980) were identified (Figs. 1, 2). Some ossicles show pentameral stereom symmetry, and many are constructed from more than one microstructural type. The pore space in these fossils was occupied by stroma during the animal's life and is now filled with cement.

Identification of mineral phases present in the ossicles was attempted by XRD analysis using a Huber Guinier X-ray powder diffractometer in transmission geometry. Entire ossicles were powdered, mixed with a silicon internal standard, and ground finely under alcohol. The instrument used Cu$K\alpha_1$ radiation at 30 kV, 20 mA. A computer-controlled point counter measured radiation counts for 100 seconds at stepped diffraction angles of 0.01° 2θ. Peak characteristics were analyzed using the curve-fitting program ORIGIN and calibrated against the silicon internal standard. The 10.4 X-ray peaks of calcite, Mg calcite, and ferroan calcite were indistinguishable, but the isolated 10.4 dolomite peak of weak intensity was identified in some samples. The four carbonate phases that occur in the fossil echinoderms were identified by electron microprobe and backscatter scanning electron microscope analyses.

Energy dispersive electron microprobe analysis allowed the differentiation of stereom from its cement fill and was conducted on the samples using a Cameca SX50 microprobe, accelerating potential = 20 kV, beam current between 3 and 5 nA, and a beam diameter between 5 and 10 μm. Minimum detection limits for Mg, Fe, and Mn are 1200 ppm. Each ossicle was analyzed on ~10 isolated spots on the stereom and ~5 spots on the cement. The location of analysis spots was checked after analysis by observing circular discoloration marks on the samples, and any data from spots that overlapped stereom and cement were rejected. The area of each analysis spot is larger than any textural irregularities identified in the stereom (Fig. 2F). An individual spot analysis is either from single-phase Mg calcite or from a mixture of calcite, Mg calcite, and dolomite.

RESULTS

$MgCO_3$ Content.—The range in mole% $MgCO_3$ from spot analyses of individual fossil echinoderm ossicles is variable (Table 2). The stereom of

JOURNAL OF SEDIMENTARY RESEARCH, VOL. 74, NO. 3, MAY, 2004, P. 355–365
 1527-1404/04/074-355/$03.00

TABLE 1.—*List of samples analyzed.*

No.	Des	Location	Stage	Paleolatitude	Age	Collector/Museum
62	c	Clapham, London, U.K. (3)	Ypresian	47°	53	A.Smith Nat Hist Mus.
10	c	Speeton, Lincolnshire, U.K. (2)	Albian	41°	100	A.Smith Nat Hist Mus.
39	l	Speeton, Lincolnshire, U.K. (2)	Hauterivian	37°	130	A.Smith Nat Hist Mus.
17	c	Santa Cruz, Portugal. (2)	Kimmeridgian	29°	152	E.Harper
29	B.s	Jarcenay, Douds, France. (3)	Oxfordian	32°	156	A.Smith Nat Hist Mus.
61	c	Huggits Wood, Yorkshire, U.K. (2)	Callovian	39°	164	J.A.D.Dickson
32	c	Whatton Cliff, Dorset, U.K. (2)	Bathonian	36°	166	J.A.D.Dickson
47	B.s	Staithes, Yorkshire, U.K. (2)	Domerian	40°	184	A.Smith Nat Hist Mus.
38	c	Cheltenham, Gloustershire, U.K. (3)	Pliensbachian	36°	190	A.Smith Nat Hist Mus.
101	c	Staithes, Yorkshire, U.K. (2)	Pleinsbachian	39°	192	J.A.D.Dickson
94	c	Black Ven, Dorset, U.K. (2)	Sinemurian	32°	200	E.Harper
90	E.c	Dolomites, Italy, (2)	Norian	25°	220	J Wendt
97	c	Djebel Tabago, Tunisia, (1)	Wordian	−4°	253	D. Erwin Smithsonian
83	c	Callythyra Springs, Australia. (2)	Artinskian	−37°	260	P Jell
98	c	Ponotoclo Co. Oklahoma, U.S.A. (1)	Virgilian	−4°	291	D.Erwin Smithsonian
102	A&c	Dry Canyon, New Mexico, U.S.A. (7)	Virgilian	−3°	292	J.A.D.Dickson
93	c	Palo Pinto Co. Texas, U.S.A. (1)	Virgilian	−3°	292	A.Molineux Tx. Mem M.
99	c	Pittsberg, Kansas, U.S.A. (1)	Desmoinesian	−3°	297	D.Erwin Smithsonian
103	c	Ozarks, Arkansas, U.S.A. (3)	Amsbergian	−13°	325	J.A.D.Dickson
70	Ag	Confusion range, Nevada, U.S.A. (2)	Chesterian	−7°	326	S Marcus Indiana Univ.
68	c	Liuzhou, Guangxi, China. (2)	Visean	−1°	330	S Marcus Indiana Univ.
41	c	Clattering Sike, Yorkshire, U.K. (3)	Brigantian	7°	330	A.Smith Nat Hist Mus.
34	c	Angle Bay, Pembrokeshire, U.K. (2)	Hastarian	−9°	350	J.A.D.Dickson
66	c	Boy Scout Camp, Indiana, U.S.A. (2)	Osagian	−18°	354	S Marcus Indiana Univ.
76	c	Button Mold Knob, Kentucky, U.S.A. (3)	Osagian	−24°	354	S Marcus Indiana Univ.
77	c	Deam Lake, Borden, Indiana, U.S.A. (2)	Osagian	−18°	354	S Marcus Indiana Univ.
26	L.m	Eiffel, Germany. (1)	M. Devonian	−8°	385	A.Smith Nat Hit Mus.
104	c	Ningqiang, Sichuan, China. (7)	Telychian	−12°	432	Y.Li
30	c	Jasper National Park, Canada. (3)	Botomian	18°	518	N.Butterfield

No. = sample number. Des = sample designation: c = crinoid, I = *Isocrinus*, A&c = *Archaeocidaris* and crinoid, L.m. = *Lepidocrinus multi*, B.s. = *Balanocrinus solentois*, E.c. = *Encrinurus cassianus* and Ag = *Agassizocrinus*. Paleolatitude = estimated using "Time Trek-4" (Cambridge Paleomap Services Ltd.) Age = age in Ma. Number of ossicles analyzed in brackets.

an interambulacral plate from the modern echinoid *Echinus esculentus* was analyzed for comparative purposes: 17 spot analyses show a range of 1.6 mole% $MgCO_3$ (from 5.43 to 7.00; Table 2). Some fossil ossicles, such as two from Whatton cliff (sample 32) composed of Mg calcite have mole% $MgCO_3$ ranges that are comparable to that of modern *Echinus esculentus*: specimen 32a with 4.03%–5.80% ($n = 10$, mean 4.24%, $\sigma = 0.55$) and specimen 32b with 3.89%–4.28% ($n = 10$, mean 4.12%, $\sigma = 0.15$). Ossicles composed of calcite and microdolomite (tiny anhedral dolomite crystals) exhibit differing ranges. For example, specimen 103a has a high mean mole% $MgCO_3$ content of 9.62% ($n = 10$, $\sigma = 1.40$) and a large range 7.67 to 11.82% compared to specimen 102g, which has an even higher mean mole% $MgCO_3$ value of 11.63% but a much smaller range, 10.67% to 12.88%. The variable ranges in the transformed ossicles are likely caused by differences in the size and distribution of microdolomite crystals, as illustrated by specimen 103a in Figure 2F. Different ossicles, all from a single specimen, showing similar textures have spot analyses that tend to have similar distributions in mole% $MgCO_3$ data (Table 2). This is illustrated in histograms of spot analyses from *Echinus esculentus* and specimen 104, the sample with the most ossicle analyses (Fig. 3). The 7 ossicles from specimen 104 have similar medians and means, but with varying symmetries. For this and all specimens the mean is taken to be representative. Seven ossicles from different samples of specimen 102, and 7 ossicles from a single thin section of specimen 104 show variable mean mole% $MgCO_3$ ranges: 1.5% in the former and 1.9% in the latter. The largest intra-sample variation (3 ossicles from sample 103) is 2.4% (Table 2).

Minerological Variations.—The stereom of some fossil echinoderms is composed of calcite or Mg calcite, which is homogeneous except for diffuse bands lying subparallel to the stereom surface (Fig. 1B). The mean mole% $MgCO_3$ of these ossicles varies between 3.4% and ~8.0%. The diffuse banding is similar to the concentric pattern of organic laminae revealed in modern echinoids by etching with glutaraldehyde-EDTA (Dubois 1991).

The stereom of some other fossil ossicles is composed of calcite, Mg calcite, and microdolomite that have a finely mottled or granular texture under the petrological microscope. This is resolved using BSEM into large millimeter-size calcite crystals that enclose many microdolomite blebs (a few microns in diameter) and evenly distributed pores ~1 μm in diameter (Fig. 2F). These echinoderms have mean mole% $MgCO_3$ values from ~5.0% to 12.5%.

Textural Variations.—The stereom of a single ossicle can show both the homogeneous and granular textures in sharply defined patches (Figs. 1F, 2B) with no difference in Mg^{2+} content. In some ossicles, homogeneous patches are found in delicate portions and granular patches in coarse portions of the stereom (Fig. 1F), but in other ossicles both types are present within single ossicles of the same microstructural type (Fig. 2B). In some specimens that show variable textures there is a tendency for stereom with less than 8 mole% $MgCO_3$ to be homogeneous while that with more than 8 mole% $MgCO_3$ is granular (Fig. 2F). However, the division between homogeneous and granular textured stereom in general cannot be drawn at a precise Mg^{2+} concentration, which is not surprising, inasmuch as these randomly selected samples have undergone different diagenetic histories.

Secular Mg^{2+} Variations.—The Mg^{2+} content of fossil echinoderms rises and falls throughout the Phanerozoic. Jurassic ossicles (18) from a greenhouse epoch have mean mole% $MgCO_3$ of 4.8% with a range between 3.8% and 6.1% (Table 2) in contrast to 10 Pennsylvanian icehouse ossicles that have mean mole% $MgCO_3$ of 11.1% with a range between 9.9% and 12.5%. Many of the Jurassic ossicles, and none of the Pennsylvanian ossicles, are partly preserved in Mg calcite. Unsurprisingly, the Carboniferous, more unstable, ossicles have all transformed to calcite and microdolomite. High Mg^{2+} values are recorded from Cambrian, Permian, and Triassic ossicles and low values from Cretaceous and Paleogene ossicles, but the number of analyses per period is small (Table 2).

Fe^{2+} and Mn^{2+} Variations.—The stereom of most ossicles have Fe^{2+} and Mn^{2+} concentrations close to or below the detection limits of 1200 ppm (Table 2). The stereom pores are usually filled with ferroan calcite (0.8–3.0% Fe), but pyrite, siderite, and manganoan calcite also occur; these phases are absent from the stereom.

DISCUSSION

Echinoderm Skeletal Preservation

Evidence exists for the rapid stabilization of Mg calcite; skeletal Mg calcite loses half its Mg concentration in 10^1–10^3 yr (Patterson and Walter

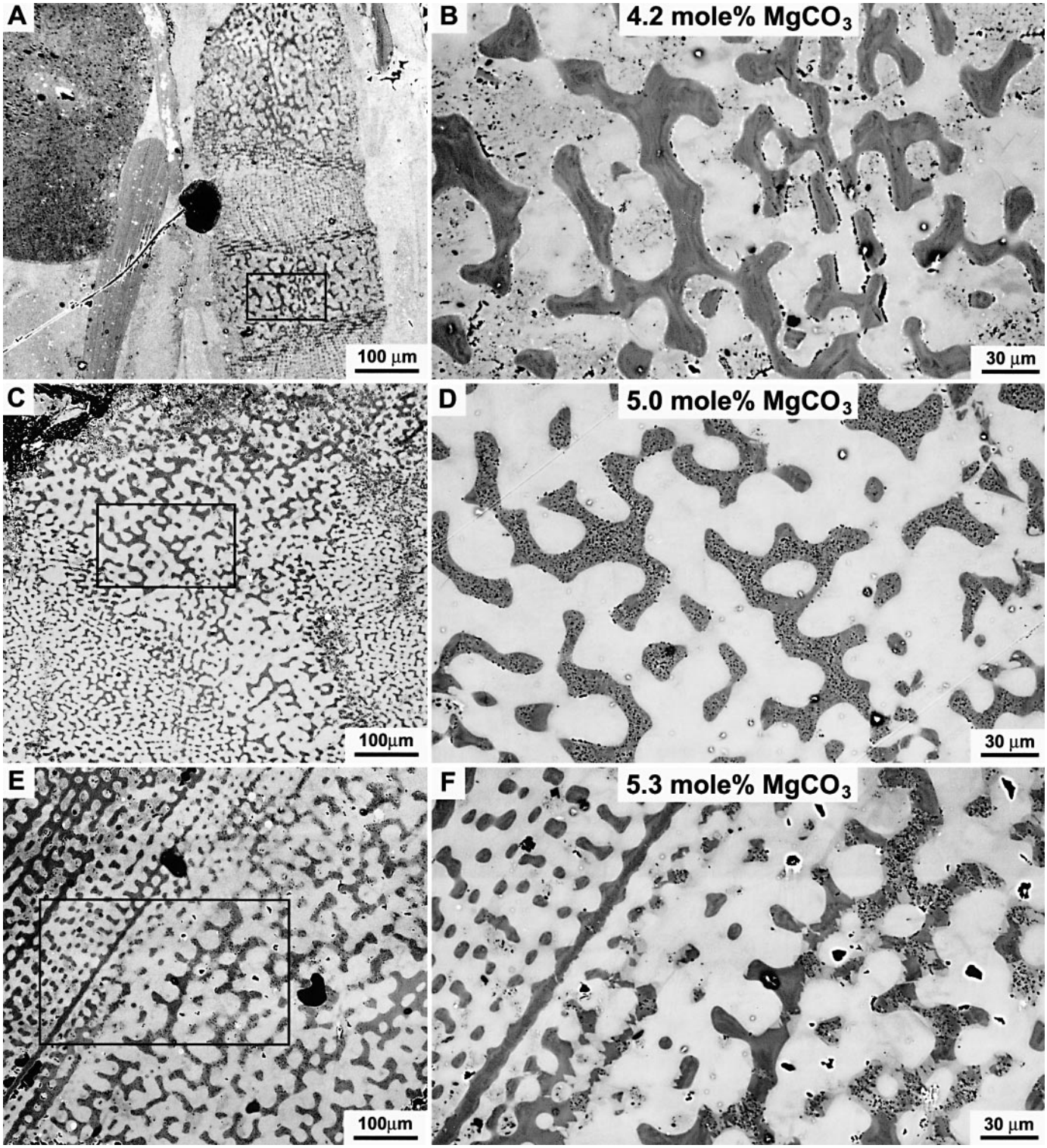

FIG. 1.—Paired SEM backscatter images of samples showing stereom microstructure. Box on A, C, and E are enlarged on B, D, and F, respectively. Average mole% $MgCO_3$ of stereom is given at top of B, D, and F images. **A)** Crinoid ossicle from Forest Marble, Dorset, U.K., specimen 32. Bands of fine rectilinear and coarse labyrinthic stereom (dark gray), in ossicle center right. **B)** Labyrinthic stereom composed of nonporous Mg calcite (dark gray with ''swirling'' lines). Calcite cement is mottled white and pale gray with sporadic pores. Pores are present along some contacts between stereom and cement. **C**) Portion of crinoid ossicle from Staithes Sandstone Yorkshire, U.K., specimen 101. Labyrinthic stereom is dark gray and ferroan calcite cement is white. This ossicle has five rays of coarser stereom, although only one is shown in this figure (lower right to upper left) that radiates from an axial canal. **D)** Stereom has finely mottled pattern composed of calcite (gray), dolomite (dark gray) and micropores (black spots). Uniform white area is cement composed of ferroan calcite. **E)** Crinoid ossicle from Lias, Cheltenham, U.K., specimen 38. Galleried stereom forming center of ossicle (upper right), labyrinthic stereom forming periphery of ossicle (lower left). **F)** Galleried stereom composed of nonporous Mg calcite (uniform dark gray); labyrinthic stereom composed of patches of nonporous stereom and patches of finely mottled stereom composed of calcite, dolomite with many micropores. Palest gray area is ferroan calcite cement.

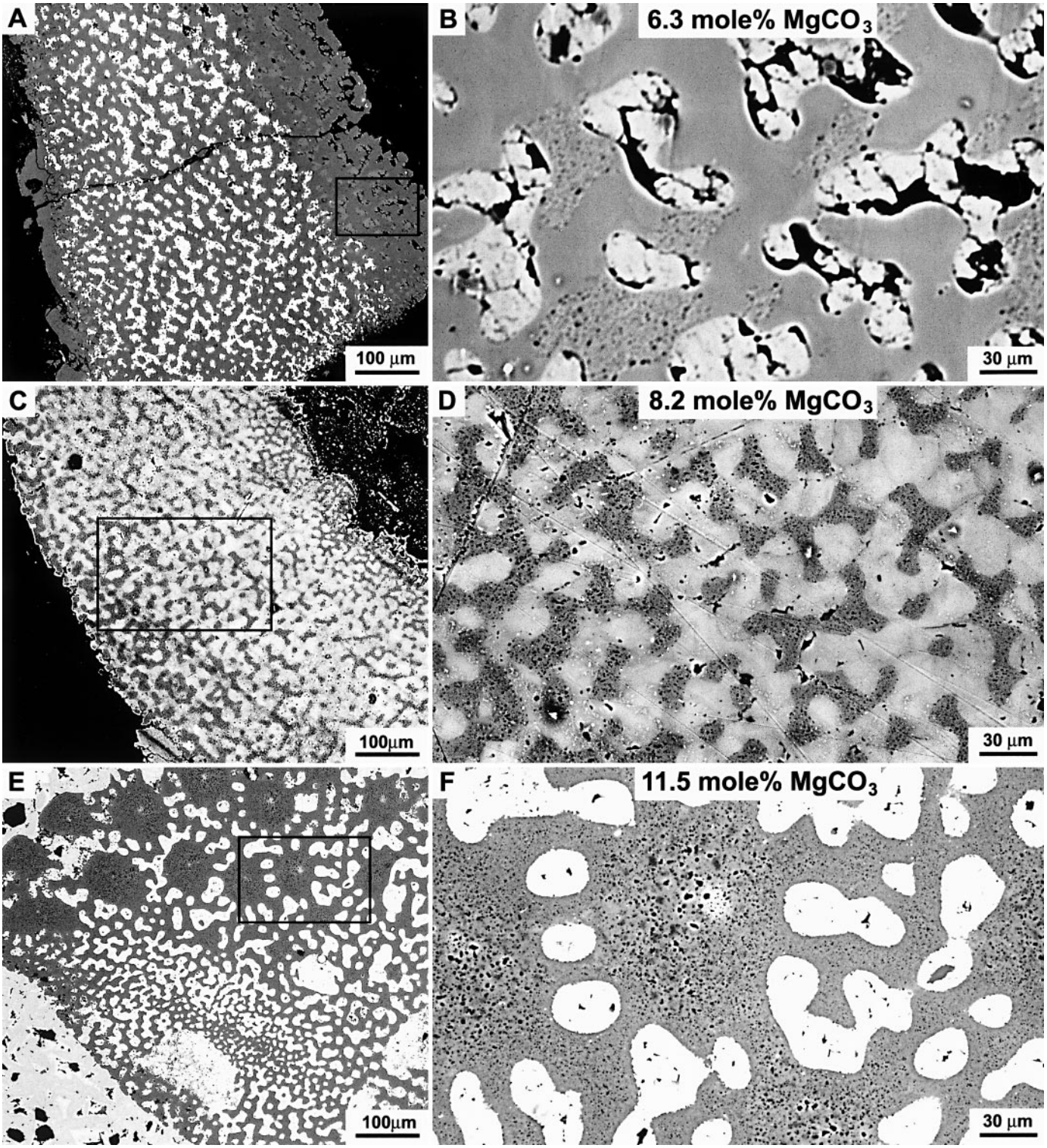

FIG. 2.—Paired SEM backscatter images of samples showing stereom microstructure. Box on A, C, and E are enlarged on B, D, and F, respectively. Average mole% $MgCO_3$ of stereom is given at top of B, D, and F images. **A)** Portion of *Isocrinus* ossicle from Speeton Clay, Lincolnshire, U.K., specimen 39. Stereom is dark gray; skeletal pores at center of ossicle filled with pyrite (white). Margin of ossicle is composed of dark gray stereom and cement that is a slightly lighter shade of gray. **B)** Stereom composed of patches of Mg calcite (uniform gray) and mottled areas of calcite (gray), dolomite (dark gray), and many micropores (black). Original stereom pores are now occupied by small ferroan calcite crystals (palest gray) and irregular shaped pores (black). **C)** Portion of circular crinoid stem ossicle with axial canal to upper right, Clattering Sike, Yorkshire, U.K., specimen 40. Labyrinthic stereom (gray), and ferroan calcite cement (pale gray). **D)** Labyrinthic stereom composed of calcite (gray), dolomite (dark gray) with many micropores (black). Ferroan calcite cement is palest gray. **E)** Echinoderm ossicle with complex stereom (dark gray) pattern, Imo Formation, Arkansas, U.S.A., specimen 103. Stereom pores and intergranular pore (lower left) are filled with zoned siderite (white) cement. Pale spots at center of coarse stereom trabeculae (upper half) are artifacts caused by microprobe beam. **F)** Stereom composed of calcite (dark gray), dolomite (darker gray spots), and many micropores (black). The micropores and dolomite blebs at the center of coarse stereom are larger than those in the areas of thinner stereom. Pale spot about 10 μm in diameter just above center is discoloration mark caused by microprobe beam. Skeletal pores are filled by siderite cement crystals (white).

TABLE 2.—*Elemental data from interambulacral plate of modern* Echinus esculentus *(*E.e*.) and the stereom of 70 fossil echinoderm ossicles. List is organized in order of increasing Mg^{2+} content of fossils.*

No.	Fe%	Mn%	No. of Spot Analyses	Ca% Range	Ca% Av s.d.	Mg% Range	Mg% Av s.d.	Mole% $MgCO_3$	Seawater Mg/Ca
E.e	x	x	17	33.14–36.40	35.68 (0.78)	1.33–1.72	1.50 (0.10)	6.1 (0.4)	1.8 (0.1)
10a	x	0.14	10	37.34–38.64	37.96 (0.42)	0.56–1.21	0.84 (0.21)	3.4 (0.8)	0.9 (0.3)
10b	x	0.19	10	37.81–39.01	38.49 (0.55)	0.65–1.39	0.85 (0.23)	3.5 (0.9)	0.9 (0.3)
61a	x	x	10	36.54–38.04	37.53 (0.52)	0.64–1.14	0.91 (0.15)	3.7 (0.6)	1.0 (0.2)
32b	x	x	10	35.39–36.24	35.78 (0.29)	0.95–1.05	1.01 (0.04)	4.1 (0.1)	1.2 (0.1)
61b	x	x	9	37.62–38.92	38.20 (0.46)	0.87–1.42	1.06 (0.20)	4.3 (0.8)	1.2 (0.2)
29a	x	x	10	35.60–38.73	37.49 (0.84)	0.99–1.15	1.07 (0.05)	4.4 (0.2)	1.2 (0.1)
94a	x	x	11	37.63–38.13	37.92 (0.24)	0.90–1.65	1.07 (0.21)	4.4 (0.8)	1.2 (0.2)
94b	x	x	10	36.94–38.48	37.80 (0.43)	0.86–1.23	1.80 (0.11)	4.4 (0.4)	1.2 (0.1)
29c	x	x	11	36.90–38.43	37.60 (0.48)	0.82–1.45	1.10 (0.18)	4.5 (0.7)	1.3 (0.2)
47a	x	x	11	36.54–37.98	37.52 (0.26)	0.95–1.42	1.13 (0.12)	4.6 (0.5)	1.3 (0.1)
76c	x	x	10	37.21–38.34	37.79 (0.33)	1.00–1.59	1.16 (0.19)	4.7 (0.8)	1.3 (0.2)
77b	x	x	6	37.24–38.07	37.67 (0.28)	0.94–1.44	1.17 (0.20)	4.8 (0.8)	1.3 (0.2)
29b	x	x	10	36.85–38.15	37.58 (0.36)	0.87–1.53	1.19 (0.18)	4.9 (0.7)	1.4 (0.2)
101a	x	x	15	36.64–37.39	36.91 (0.30)	0.82–1.17	1.20 (0.18)	4.9 (0.7)	1.4 (0.2)
77a	x	x	9	36.85–38.61	37.97 (0.55)	0.82–1.43	1.20 (0.20)	4.9 (0.8)	1.3 (0.2)
32a	x	x	10	34.81–36.64	35.51 (0.52)	0.99–1.66	1.22 (0.14)	5.0 (0.6)	1.5 (0.2)
38a	x	x	9	36.33–36.98	36.55 (0.23)	1.05–1.35	1.24 (0.09)	5.0 (0.4)	1.5 (0.1)
17b	x	x	7	36.54–37.61	37.03 (0.41)	1.15–1.32	1.25 (0.12)	5.1 (0.5)	1.5 (0.1)
62a	x	x	14	33.42–37.12	35.51 (1.13)	1.12–1.47	1.28 (0.13)	5.2 (0.6)	1.5 (0.2)
62b	0.59	x	5	34.90–35.94	35.42 (0.40)	0.95–1.50	1.28 (0.20)	5.2 (0.8)	1.6 (0.2)
17a	x	x	10	34.41–38.41	37.23 (0.62)	0.92–1.98	1.30 (0.32)	5.3 (1.3)	1.5 (0.4)
38b	x	x	8	36.43–36.90	36.74 (0.16)	1.12–1.44	1.31 (0.10)	5.3 (0.4)	1.5 (0.1)
47b	x	x	10	36.08–37.06	36.70 (0.33)	1.05–1.53	1.31 (0.15)	5.4 (0.6)	1.6 (0.2)
101b	x	x	15	35.94–37.38	36.91 (0.39)	0.96–1.68	1.33 (0.22)	5.4 (0.9)	1.5 (0.3)
66b	x	x	10	38.58–39.19	39.06 (0.03)	1.13–1.74	1.35 (0.18)	5.5 (0.7)	1.5 (0.2)
76b	x	x	10	36.66–38.36	37.43 (0.49)	0.93–1.83	1.36 (0.32)	5.5 (1.3)	1.6 (0.4)
76a	x	x	10	37.17–38.55	37.79 (0.47)	0.96–1.78	1.38 (0.25)	5.6 (1.0)	1.6 (0.3)
66a	x	x	10	37.69–38.85	38.08 (0.33)	1.31–1.66	1.47 (0.10)	6.0 (0.4)	1.7 (0.1)
38c	x	x	5	35.95–37.12	36.77 (0.48)	1.35–1.63	1.49 (0.10)	6.1 (0.4)	1.8 (0.1)
34a	0.23	x	10	36.28–38.33	37.52 (0.80)	1.08–1.97	1.49 (0.40)	6.1 (1.6)	1.7 (0.5)
39b	0.29	x	10	35.69–37.25	36.32 (0.48)	1.37–1.69	1.52 (0.02)	6.2 (0.4)	1.7 (0.1)
39a	x	x	10	35.68–37.89	36.73 (0.65)	1.12–2.31	1.54 (0.41)	6.3 (1.6)	1.8 (0.5)
104d	x	x	10	37.19–38.41	37.71 (0.42)	1.49–1.90	1.64 (0.13)	6.7 (0.5)	1.9 (0.1)
62c	x	x	10	37.04–37.78	37.30 (0.24)	1.57–1.81	1.65 (0.09)	6.7 (0.4)	1.9 (0.1)
104g	x	x	10	37.27–38.62	37.70 (1.11)	1.52–1.87	1.69 (0.11)	6.9 (0.5)	1.9 (0.1)
104f	x	x	10	36.92–38.68	37.97 (0.58)	1.43–1.89	1.69 (0.17)	6.9 (0.7)	1.9 (0.2)
104a	x	x	10	37.19–40.21	38.52 (0.79)	1.39–2.07	1.74 (0.20)	7.0 (0.8)	1.9 (0.2)
68b	x	x	10	36.97–38.07	37.45 (0.41)	1.48–2.32	1.77 (0.26)	7.2 (1.1)	2.0 (0.3)
68a	x	x	10	37.83–38.76	37.85 (0.04)	1.48–2.53	1.79 (0.32)	7.3 (1.3)	2.0 (0.4)
34b	0.15	x	10	35.92–38.19	37.15 (0.76)	1.19–3.02	1.83 (0.59)	7.4 (2.3)	2.1 (0.7)
83a	x	x	8	36.49–37.68	37.02 (0.46)	1.78–2.11	1.90 (0.10)	7.7 (0.4)	2.2 (0.1)
41b	x	x	10	36.43–37.95	36.96 (0.45)	1.49–2.27	1.93 (0.23)	7.8 (0.9)	2.2 (0.3)
104c	x	x	21	36.66–38.23	37.46 (0.38)	1.40–2.51	1.95 (0.38)	7.9 (1.5)	2.2 (0.4)
104e	x	x	10	37.10–38.44	37.80 (0.42)	1.74–2.43	2.02 (0.23)	8.2 (0.9)	2.3 (0.3)
41a	x	x	10	36.23–37.94	37.30 (0.60)	1.46–3.02	2.03 (0.59)	8.2 (2.3)	2.3 (0.7)
26a	x	x	11	35.96–38.43	37.16 (0.63)	1.19–3.04	2.05 (0.55)	8.3 (2.2)	2.4 (0.7)
83b	x	x	11	35.72–37.06	36.82 (0.60)	1.73–2.66	2.09 (0.31)	8.5 (1.3)	2.5 (0.4)
104b	x	x	10	37.96–39.04	38.58 (0.34)	1.91–2.49	2.11 (0.19)	8.6 (0.8)	2.4 (0.2)
41c	x	x	9	35.96–37.40	36.76 (0.50)	1.87–2.67	2.19 (0.30)	8.9 (1.2)	2.6 (0.4)
70a	x	x	10	37.05–37.90	37.36 (0.24)	1.85–2.73	2.22 (0.27)	9.0 (1.1)	2.6 (0.3)
103a	x	x	8	35.67–38.15	36.89 (0.90)	1.89–2.93	2.37 (0.35)	9.6 (1.4)	2.8 (0.5)
97a	x	x	9	35.55–39.25	37.38 (1.14)	1.56–3.45	2.38 (0.66)	9.6 (2.6)	2.9 (0.8)
98a	x	x	11	36.48–38.78	37.46 (0.68)	1.32–3.27	2.45 (0.63)	9.9 (2.5)	2.8 (0.8)
102a	0.13	x	11	34.48–36.93	35.86 (0.67)	1.82–3.24	2.50 (0.42)	10.1 (1.7)	3.0 (0.6)
102c	x	x	8	35.32–38.24	36.10 (0.95)	2.11–3.11	2.55 (0.37)	10.3 (1.5)	3.0 (0.5)
30b	0.18	0.20	10	33.86–36.49	35.26 (0.93)	1.92–4.00	2.56 (0.64)	10.3 (2.6)	3.1 (0.9)
30c	0	0.18	10	35.00–36.78	35.72 (0.51)	2.15–3.33	2.61 (0.36)	10.6 (1.4)	3.2 (0.5)
70b	x	x	11	37.01–38.28	37.62 (0.44)	2.02–3.40	2.64 (0.38)	10.7 (1.5)	2.5 (0.5)
102d	x	x	3	35.93–36.31	36.00 (0.28)	2.56–2.77	2.69 (0.12)	10.9 (0.5)	3.2 (0.1)
102e	x	x	7	35.85–38.64	36.72 (1.00)	2.18–3.03	2.73 (0.27)	11.0 (1.1)	3.2 (0.3)
30a	0.16	0.18	10	33.16–36.04	35.36 (0.09)	2.11–4.65	2.73 (0.08)	11.0 (3.1)	3.4 (1.1)
102b	x	x	12	34.44–36.84	35.34 (0.71)	2.17–3.25	2.78 (0.43)	11.2 (1.7)	3.4 (0.6)
102f	x	x	10	34.50–36.30	35.15 (0.66)	2.20–3.30	2.81 (0.37)	11.3 (1.5)	3.4 (0.5)
90a	x	x	10	35.52–37.33	36.20 (0.57)	2.34–3.23	2.82 (0.32)	11.4 (1.3)	3.4 (0.4)
93a	x	x	8	36.34–36.82	36.61 (0.15)	2.76–3.02	2.87 (0.10)	11.6 (0.4)	3.4 (0.1)
103b	x	x	7	36.06–36.35	36.16 (0.11)	2.74–2.94	2.87 (0.06)	11.6 (0.3)	3.4 (0.1)
102g	x	x	10	34.58–35.01	34.87 (0.19)	2.61–3.20	2.88 (0.17)	11.6 (0.7)	3.6 (0.2)
90b	x	x	9	36.77–37.18	37.03 (0.23)	2.74–3.39	2.96 (0.19)	11.9 (0.8)	3.4 (0.2)
103c	x	x	10	35.22–35.86	36.08 (0.38)	2.50–3.32	2.98 (0.29)	12.0 (1.1)	3.6 (0.4)
99a	x	x	10	34.82–37.30	36.17 (0.67)	2.83–4.23	3.11 (0.52)	12.5 (2.0)	3.7 (0.7)

No. = sample number, Seawater Mg/Ca calculated using partition coefficient $D^cMg^{2+} = 0.03757$, and x = below detection limit.

1994; Budd and Hiatt 1993). Mg calcite when bathed in meteoric water can be totally dissolved (Budd 1992), stabilized in 10^5 yr (Land et al. 1967), or stabilized with a half-life of 60 kyr (Lafon and Vacher 1975). The impression given by these works is that Mg calcite is rapidly removed from the geological record, a view reinforced for echinoderms by Weber (1969), who found only one Pleistocene example from ~1800 fossil echinoderms that contained more than a few percent Mg^{2+}. However, echinoderms preserved in Mg calcite are reported here from rocks as old as the Silurian (Table 2). The stereom microstructure of such ossicles is perfectly defined, and they appear homogeneous on BSEM images (Fig. 1B). These echi-

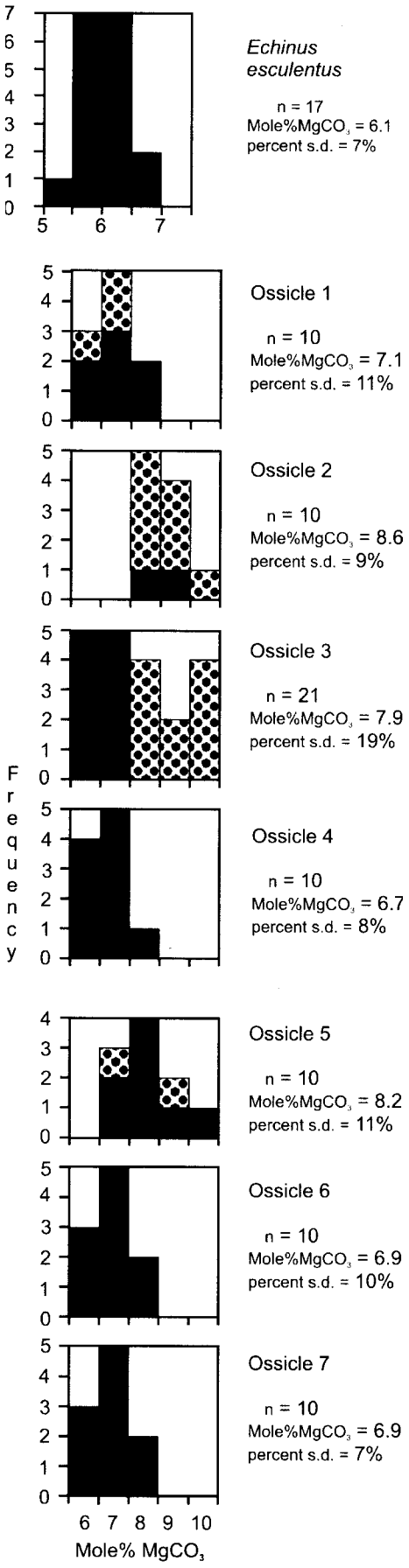

noderms still possess high diagenetic potential but have remained unaltered because they occur in fine-grained sediments of low permeability and their pores were sealed early in their history by cement, preventing fluid access to the ossicles' interior.

Fossil echinoderms generally have been transformed to calcite and microdolomite with a wide range of textures (Dickson 2001b). Commonly their stereom microstructure is poorly preserved, and they consist of dolomite crystals that are microrhombic set homoaxially in large calcite crystals (Richter 1974; Lohmann and Meyers 1977). Some of the echinoderms reported in Table 2 that have transformed to calcite and microdolomite, however, still posses well defined stereom microstructure and their trabeculae are constructed of dolomite blebs (a few microns in diameter) set randomly in calcite (a few millimeters in diameter; Figs. 1, 2). These echinoderms are texturally identical to modern echinoid ossicles that have been experimentally transformed by heating (Gaffey et al. 1991; Dickson 2001a). The range in mole% $MgCO_3$ recorded from spot analyses of individual fossil echinoderm ossicles (Table 2) indicates that Mg^{2+} redistribution probably took place over tens of microns during transformation, but this redistribution was confined to the stereom as the stereom–cement contacts remain sharply defined. The presence of diffuse primary growth banding in a Carboniferous ossicle from specimen 102 (visible in cathodoluminescence) indicates Mn^{2+} movement of no more than a few microns over the last ~300 Myr (Dickson 2001b).

Mg Content of Stereom

Abundant data exist for the Mg^{2+} content of modern echinoderms in relationship to temperature (Fig. 4), a correlation noted by Chave (1954). Weber (1969, 1973) analyzed echinoderms for Mg^{2+} from polar to tropical seas and from shallow to abyssal waters. He found systematic variation between the various skeletal elements of single echinoid tests and between different genera under the same environmental conditions and thought that the variation was due to genetic and environmental factors. The spread of data and low R^2 value (0.455) for echinoderm data plotted in Figure 4 is probably due to physiological effects. Modern marine Mg calcite cements and echinoderms have the same range of Mg^{2+} compositions, and both are similarly correlated with temperature (Fig. 4). These relationships are in sharp contrast to planktonic foraminifera, which discriminate strongly against Mg^{2+} (Fig. 4) when producing their calcite tests (Hastings et al. 1998).

The fossil echinoderms used in this study come from sediment deposited in shallow marine waters mostly located in subtropical to tropical paleolatitudes (specimen 62, at 47° N is farthest from an estimated paleo-equator; Table 1) at temperatures probably between 20°C and 30°C. Modern tropical echinoids that live between 30° N and 30° S of the Equator in waters of 23–29°C can be compared with these fossils. They produce coronal plates with a mole% $MgCO_3$ range of 7 (11.9–19.3%) and a mean of 16% (n = 62; Weber 1973).

Phanerozoic Carbonate Mineralogy

Secular Variation in Carbonate Mineralogy.—Identification of the dominant abiotic carbonate phase to precipitate from shallow seawater has concentrated on the alternation between calcite and aragonite (Sandberg 1975; Sandberg 1983; Mackenzie and Pigott 1981; Wilkinson and Given

←

FIG. 3.—Histograms showing mole% $MgCO_3$ plotted against frequency for the modern echinoid *Echinus esculentus* and 7 echinoderm ossicles from sample 104, Ningqiang, Sichuan, China. Frequency classes are 1 mole% $MgCO_3$. Note change in scale for mole% $MgCO_3$ between *Echinus* and fossil echinoderms. Black bars = homogeneous stereom composed of Mg calcite, stippled bars = granular stereom composed of Mg calcite, calcite, and microdolomite.

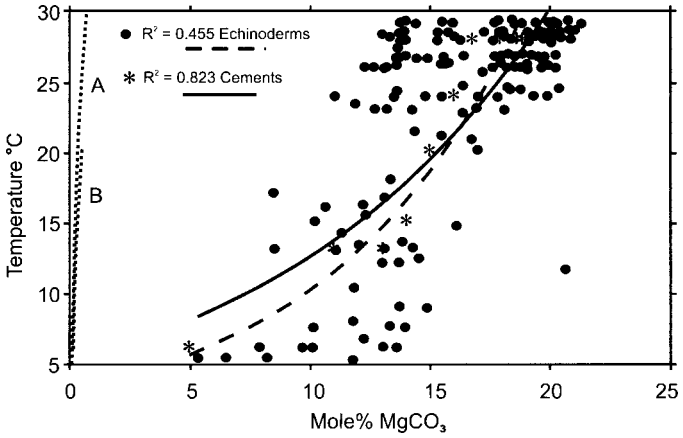

FIG. 4.—Scatter diagram of mole% $MgCO_3$ plotted against temperature for 173 modern echinoderms and 11 marine cements. Echinoderm data include analytical composition and recorded temperature from individual specimens of echinoid tests, asteroids, ophiuroids, and crinoids (Chave 1954); from average composition from coronal plates for echinoid and asteroid genera (Weber 1973); and averaged data from the tests of echinoid, asteroid, ophiuroid, and crinoid orders (Weber 1969). Cement data are from Alexandersson (1972), Ginsburg and Schroeder (1973), Milliman and Müller (1973), Müller and Fabricius (1974), James et al. (1976), Macintyre (1977), Schlager and James (1978), McKenzie and Bernoulli (1982), Pigott and Land (1986), Andrews (1988), and Carpenter et al. (1991). Curves of Mg/Ca versus temperature for planktonic foraminiferal tests are from Nürnberg et al. (1996a, 1996b) and Elderfield and Ganssen (2000), replotted as curves A and B, respectively.

1986; Lasemi and Sandberg 1984), and the role of Mg calcite has received little attention. The bulk mean composition of predominantly low-latitude fossil echinoderms reported here oscillates between 4 and 12 mole% $MgCO_3$ throughout the Phanerozoic (Fig. 5A) in phase with the proposed aragonite–calcite seas alternation. The lowest Mg^{2+} content of the 29 analyzed echinoderm samples at ~3.5% mole% $MgCO_3$ comes from two Albian ossicles (specimen 10) with one Callovian ossicle at 3.8% mole% $MgCO_3$ (specimen 61a, Table 2). Hence, even at times when calcite seas are proposed, only 3 of the 70 ossicles analyzed dip slightly below the 4 mole% $MgCO_3$ composition that is used to divide calcite from Mg calcite. This situation apparently differs with marine cements from greenhouse epochs that are composed of calcite with low Mg^{2+} contents. Woo et al. (1993), for instance, record mid-Cretaceous radiaxial calcite with less than 1 mole% $MgCO_3$. This difference between echinoderms and marine cements could be the Cretaceous norm (a situation that would differ from that today; Fig. 4); they could have formed at substantially different temperatures, or one, or both, of the samples has not preserved its original composition. Despite this difference, mole% $MgCO_3$ contents of a selection of well preserved marine Mg calcite cements plot in positions similar to echinoderm data in Figure 5A. Early Paleozoic cements contain less Mg^{2+} than contemporary ossicles.

Modern tropical echinoids have a mean value of 16.0 mole% $MgCO_3$ (Weber 1973), which is higher than any fossil echinoderm and implies that seawater Mg/Ca ratio is higher today than throughout the Phanerozoic. This is probably due, at least in part, to the formation of marine dolomite today being at an all-time Phanerozoic low (Given and Wilkinson 1987; Burns et al. 2000; Holland and Zimmermann 2000). Another factor is that the locus of marine calcium carbonate production and accumulation switched from shallow platforms to the open ocean during the late Mesozoic (Morse and McKenzie 1990). Mg calcite is formed today principally on tropical platforms while pelagic carbonates are composed mainly of calcite. The relative rise in Ca^{2+} abstraction due to increasing numbers of pelagic calcifers during the Tertiary and the long-term (10^7yr) sequestering of this Ca^{2+} in the deep ocean would cause a rise in seawater Mg/Ca ratio. The amount of Mg^{2+} abstracted from the ocean due to Mg calcite precipitation was also reduced as the area of tropical platforms decreased throughout the Tertiary (Walker et al. 2002). The effectiveness of Mg calcite as a long-term Mg^{2+} sink, however, is difficult to assess, because this Mg^{2+} is released back to the ocean during stabilization of Mg calcite to calcite (Wilkinson and Algeo 1989).

Control on marine carbonate mineralogy has recently been ascribed to the Mg/Ca ratio of seawater (Hardie 1996; Stanley and Hardie 1998; 1999; Stanley et al. 2002) but is complex and likely to be influenced by many factors (Burton 1993). While seawater Mg/Ca ratio is undoubtedly important, it is unlikely to be the only control. Indeed, Morse et al. (1997) have shown that temperature is just as important. It is sanguine that much surface seawater today is unfavorable for calcite precipitation being supersaturated with respect to aragonite with a high Mg/Ca ratio = 5.2, yet biological control overrides these factors and the dominant precipitate from today's ocean is biogenic calcite from planktonic calcifiers.

Mg/Ca Ratio of Phanerozoic Seawater

Geochemical Models.—Geochemical models for seawater Mg/Ca throughout the Phanerozoic have utilized estimates for the supply of these elements to the oceans by rivers, exchange by hydrothermal flow at mid-ocean ridge spreading centers (MORs), and removal by carbonate and evaporite precipitation. Models have been proposed for the last 100 Myr (Berner et al. 1983; Lasaga et al. 1985) and for the entire Phanerozoic (Wilkinson and Algeo 1989; Hardie 1996; Wallmann 2001). Dolomitization is a major Mg^{2+} sink that has been incorporated in some models but not in others, and even where incorporated, estimates of its secular abundance vary widely (Given and Wilkinson 1987; Holland and Zimmermann 2000). The Spencer and Hardie (1990) and Hardie (1996) model is based on the mixing ratio of river water and hydrothermal fluids generated at MORs; however, the validity of their input data has been questioned by Holland et al. (1996), Holland and Zimmermann (2000), and Rowley (2002). These geochemical models predict that the Mg/Ca ratio of seawater oscillated between 1.0 and 5.0 throughout the Phanerozoic (Fig. 5B) and is in phase with other first-order global cycles such as atmospheric CO_2 concentration, sea level, ''icehouse'' versus ''greenhouse'' conditions, and so on.

Evaporite Mineralogy and Fluid Inclusions.—The compositions of potash salts have been used to indicate secular change in seawater chemistry. According to Hardie (1996) the presence of $MgSO_4$-bearing potash evaporites coincides with times when aragonite ooids and cements are abundant and seawater Mg/Ca is high, and KCl-bearing evaporites are precipitated when aragonite is scarce or absent and seawater Mg/Ca is low.

The chemical evolution of evaporating water during halite precipitation has been monitored by analysis of sequential fluid inclusions (Zimmermann 2001; Lowenstein et al. 2001; Horita et al. 2002). The evaporation path determined from these inclusion data can be extrapolated to determine the initial composition of seawater. This is straightforward if evaporation follows the modeled path for present seawater (Harvie et al. 1984); but most natural systems are open so the effects of dolomitization (Holland et al. 1996; Holland and Zimmermann 2000; Zimmermann 2000; Brennan and Lowenstein 2002; Horita et al. 2002) and the addition of external waters (Ayora et al. 2001) before halite precipitation commences makes prediction more difficult.

Lowenstein et al. (2001) and Horita et al. (2002) have recently compiled inclusion data from halite and give an assessment of how these data can be used to reconstruct the chemistry of Phanerozoic seawater. The Horita et al. Mg/Ca curve is similar to the Kovalevich et al. (1998) curve for Soviet and European halite inclusions. Seawater Mg/Ca ratio extrapolated from fluid-inclusion data is similar to other predictions (Fig. 5B).

Mg Calcite Cement.—Marine Mg calcite cements are thought by some to be the best proxy for ancient seawater chemistry because of the absence of biological fractionation or ''vital effects'' during their precipitation, and they have been used to predict seawater Mg/Ca (Carpenter et al. 1991;

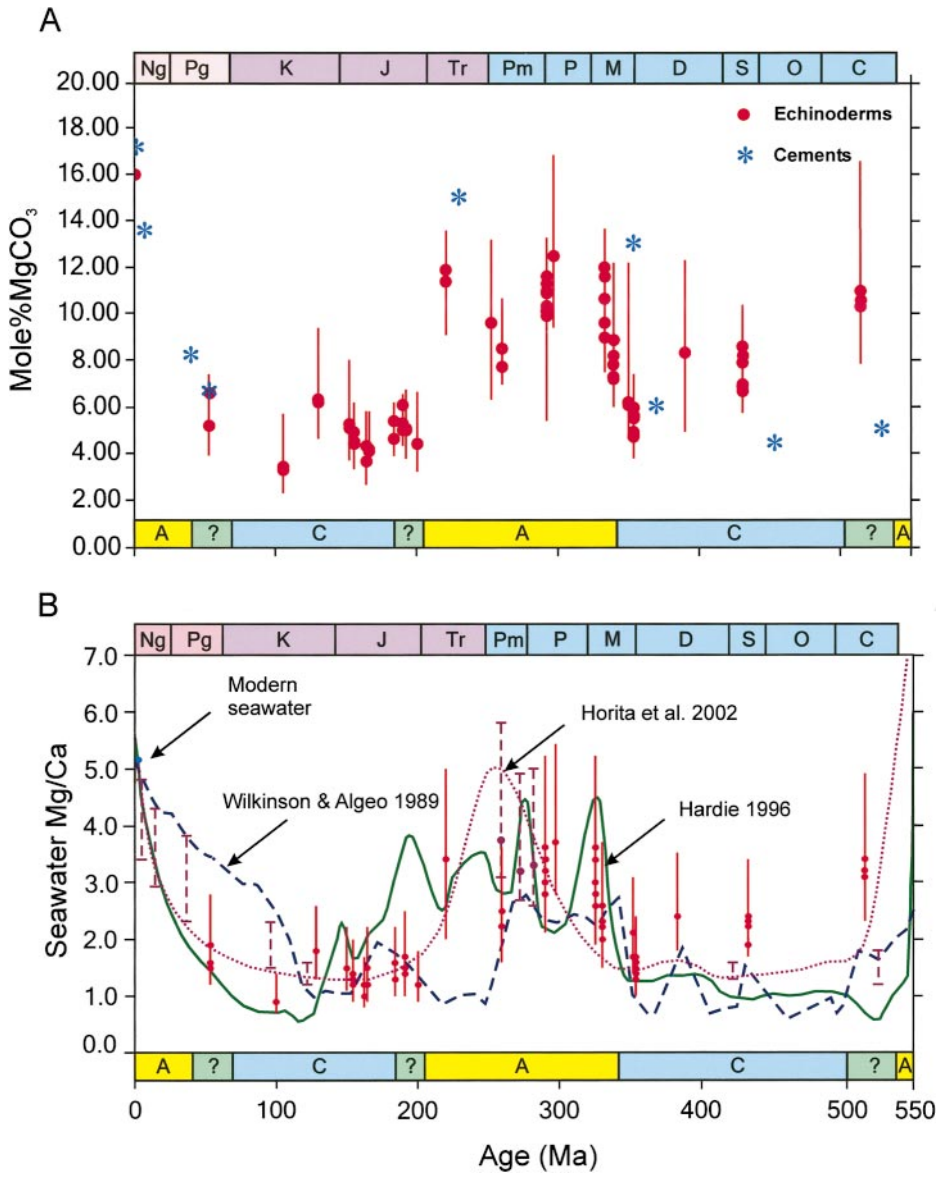

FIG. 5.—**A)** Scatter diagram of mole% $MgCO_3$ for 70 fossil echinoderm ossicles and 8 ancient Mg calcite cements plotted against age. Mean mole% $MgCO_3$ for each ossicle is shown as circle, range from spot analyses is shown as vertical line. Selected ancient Mg calcite cements (asterisks) are from Meyers and Lohmann (1978), Richter (1984), Carpenter et al. (1991), Whittaker et al. (1994), Frank and Lohmann (1996), Wilson and Dickson (1966), Tobin and Walker (1997), and Pirrie et al. (1998). Mean mole% $MgCO_3$ for modern tropical coronal echinoid stereom ($n = 62$, 16.0%) is from Weber (1973). Mean mole% $MgCO_3$ (17%) for modern tropical/subtropical Mg calcite cement is from Alexandersson (1972), Ginsburg and Schroeder (1973), James et al. (1976), Macintyre (1977), Pigott and Land (1986), and Carpenter et al. (1991). **B)** Seawater Mg/Ca molar ratio versus age. Echinoderm data are shown in red; seawater Mg/Ca ratio calculated from mean $^{m}Mg/^{m}Ca$ ratio of 70 fossil echinoderm ossicles is plotted as red dots, range on each data point is calculated from range of Mg^{2+} partition coefficients applicable to modern echinoderms (see text for details). Dashed vertical purple bars plot estimated Mg/Ca seawater range from halite fluid inclusions (Lowenstein et al. 2001; Brennan and Lowenstein 2002); the circles on three ''Permian'' bars represent estimated most likely values (Lowenstein, oral communication 2003). Dashed blue line is Mg/Ca ratio of seawater modeled by Wilkinson and Algeo (1989), solid green line is Mg/Ca ratio of seawater modeled by Hardie (1996), and dotted pink line is Mg/Ca ratio estimated from fluid-inclusion data by Horita et al. (2002). A = Aragonite Sea and C = Calcite Sea from Sandberg (1983).

Carpenter and Lohmann 1992; Cicero and Lohmann 2001). Mg calcite cements are thought to have been common, especially during icehouse epochs, but most are now altered. Evidence of alteration is sometimes obvious but can be obscure.

Magnesium Partitioning.—Prediction of seawater Mg/Ca ratios from echinoderm or Mg cement data relies on an understanding of Mg^{2+} partitioning. This has been extensively investigated between solution and synthetic calcite at 25°C, and a range of D^{c}_{Mg2+} values (0.01 to 0.05) has been assembled by Rimstidt et al. (1998). It is well established that D^{c}_{Mg2+} shows a large positive change with increasing temperature (Mucci 1987; Morse et al. 1997; Rimstidt et al. 1998), but kinetic factors such as solution Mg/Ca composition (Mackenzie et al. 1983; Mucci and Morse 1983; Hartley and Mucci 1996) affect Mg partitioning while the effect of precipitation rate and PCO_2 are controversial (Berner 1978; Given and Wilkinson 1985; Burton and Walter 1991; Mucci and Morse 1983; Hartley and Mucci 1996). A full understanding of Mg partitioning in abiotic calcite is still wanting, a fact that is clear when laboratory-derived D^{c}_{Mg2+} values determined from bulk synthetic precipitates underestimate the observed composition of modern marine Mg calcites (Mucci 1987; Morse and Bender 1990; Hartley and Mucci 1996). It has been suggested that some of these difficulties may be overcome when crystal surface effects are integrated into partitioning studies (Reeder and Grams 1987; Zhang and Dawe 2000; Davis et al. 2000), but at present the reason for this discrepancy is unknown.

Effective partition coefficients can be calculated for modern echinoderms using their Ca^{2+} and Mg^{2+} compositions and seawater Ca^{2+} and Mg^{2+} concentrations of 411 ppm and 1290 ppm, respectively. The range in mole% $MgCO_3$ for modern echinoderms living in waters of 20–30°C is 12.0–21.0% (Fig. 4), which produces partition coefficients of 0.02635 and 0.05137, respectively. These coefficients accommodate physiological effects over a 10°C range and were used to calculate the range in seawater Mg/Ca ratios indicated by mean mole% $MgCO_3$ data of the fossil data (Fig. 5B).

The large range in Mg^{2+} partitioning coefficients for all echinoderms is narrowed for individual ossicles to a single coefficient calculated from the coronal plates of modern tropical echinoids (Weber 1973). Their mean mole% $MgCO_3$ composition at 27°C is 16%, which yields a partition coefficient of 0.031819. Using this coefficient assumes that all the fossil echi-

noderms produced their skeletons at 27°C, which could be modified using temperature estimates for the fossils from paleolatitude data (Table 1). Adjustment could also be made for varying seawater Mg/Ca ratios. Fluid Mg/Ca ratio is known to influence partitioning in abiotic calcite (Mackenzie et al. 1983; Mucci and Morse 1983; Hartley and Mucci 1996), but its effect on echinoderm mineralization, while likely, is unknown at present. Rather than applying dubious corrections, the data for individual ossicles presented on Table 2 and Figure 5B (red dots) uses $D^{c}_{Mg2+} = 0.031819$. Thus, comparisons can easily be made but with the understanding that some uncertainty surrounds these calculations.

Echinoderm Data.—Despite uncertainties in applying distribution coefficients to fossil echinoderms, the seawater Mg/Ca ratio these coefficients predict follows the two first-order Phanerozoic oscillations between 1 and 5 that other methods predict (Fig. 5B). The greatest disparity between seawater Mg/Ca ratios from echinoderm and other predictions is in the early Paleozoic. Early Cambrian fibrous calcite cements were used by Whittaker et al. (1994) to estimate seawater Mg/Ca ratio = 1.4, and Lowenstein et al. (2001) used fluid inclusions from early Cambrian halite to predict a ratio of ~1.2, whereas the echinoderm data presented here indicate a ratio of 3.3. This difference in estimates may be caused by inaccurate dating. The error in age assignment on some of this data is unknown and on echinoderms is ~±3 million years. The rate of change in the Mg/Ca ratio of early Cambrian seawater is predicted to change very rapidly (Fig. 5B), so small errors in dating of samples will lead to large differences in Mg/Ca ratio estimates.

The rate of change in seawater Mg/Ca ratio during the Silurian is estimated to be small (Fig. 5B), but the value of that ratio predicted by various methods differs considerably: fluid-inclusion data (Brennan and Lowenstein 2002) indicate a ratio of 1.3 to 1.6, the echinoderm data (Table 2) indicate a ratio of 1.9 to 2.3, and calcite cements (Cicero and Lohmann 2001) indicate a ratio of ~0.2.

Carboniferous echinoderm data show a rapid rise in Mg/Ca during the early Mississippian with high Mg/Ca values from late Mississippian through late Pennsylvanian to Permian times. These data correspond in a general way with other predictions but are insufficient to verify the complex pattern proposed for the Carboniferous by the Hardie (1996) curve.

Echinoids from the Cassian (Triassic) beds of Italy indicate Mg/Ca = 3.5, which is close to the Hardie curve but far from the Wilkinson and Algeo curve (Fig. 5B), which is supported by Middle Triassic calcite cements from Sicily with a Mg/Ca ratio of 0.9 (Cicero and Lohmann 2001). The occurrence of Triassic aragonite cements (Kostecka 1972; Scherer 1977; Wood et al. 1999), however, suggests that a Mg/Ca ratio higher than 1.0 is likely.

A major difference in Mg/Ca estimates occurs in the early Jurassic when Hardie's (1996) model indicates a Mg/Ca ratio of 3.0 in the early Jurassic, but this does not correspond with any of the other estimates, which are ~1 for the early Jurassic (Fig. 5B).

The single echinoderm sample from the Cenozoic (Mg/Ca = 1.7) is consistent with Hardie's Mg/Ca curve (1996) and data from fluid-inclusions (Zimmerman 2000) and benthic foraminifera (Lear et al. 2000).

CONCLUSIONS

Fossil echinoderms are preserved in a plethora of different ways. The stereom pore system of some ossicles becomes filled with stable ferroan calcite cement before any alteration of the skeleton occurs. These cement crystal caskets have achieved preservation of some Mg calcite skeletons for 400 Myr and confined the alteration of others to within their skeletons. The distinction of stereom microstructure from cement fill in these ossicles is sharp and readily visible on BSEM images. Preservation of this highly distinctive stereom makes the task of selecting fossil echinoderms for reconstructing ocean chemistry relatively easy.

The skeletal Mg^{2+} composition of 29 marine echinoderms rises and falls in phase with other first-order global cycles. Jurassic greenhouse ossicles have low mole% $MgCO_3$ compositions (4–6%) and are often preserved as Mg calcite whereas Pennsylvanian icehouse ossicles have high mole% $MgCO_3$ compositions (9–12%) and all have stabilized to calcite and microdolomite. The lowest mean Mg^{2+} composition found for fossil echinoderms is ~3.5 mol% $MgCO_3$; hence (following the definition of Mg calcite as containing > 4 mol% $MgCO_3$) most echinoderm skeletons were composed of Mg calcite, even during times of calcite seas.

The change in seawater Mg/Ca ratio, as predicted for the Phanerozoic by geochemical models, has recently been reinforced by fluid-inclusion studies. Echinoderms now add another independent line of evidence that collectively can leave little doubt that major changes in the seawater Mg/Ca ratio have occurred. These independent lines of evidence all indicate that seawater Mg/Ca ratio varied between 1 and 5 throughout the Phanerozoic, but they differ substantially when changes over shorter time intervals (10^7yr) are considered. These differences need resolving.

This pilot study has shown the potential of echinoderms as Mg/Ca archives, but the number of analyses is inadequate to achieve statistically significant results. Analyses of many echinoderms from single samples and further samples of the same age are required. Fossil echinoderms are abundant, and examples of the required type have been recorded, particularly in paleontological literature (e.g., Savarese et al. 1996) but are as yet unanalyzed.

The prediction of seawater Mg/Ca ratios from echinoderms has advantages—their distinctive microstructure enables their diagenetic state to be easily recognized, and they provide empirical evidence as they are precipitated directly from seawater—but also disadvantages; our understanding of elemental partitioning during stereom formation is rudimentary, making accurate prediction of seawater Mg/Ca ratios uncertain.

Well preserved fossil echinoderms are an underutilized empirical archive of ancient seawater chemistry. Not only should accurate monitoring of seawater Mg/Ca ratio be possible, but the determination of latitudinal temperature variations for specific time intervals from Mg/Ca data should also be feasible. Environmentally sensitive elements such as Sr^{2+} and SO_{4-} could also be investigated, but their distribution after transformation is different from Mg^{2+} (Dickson 2001b) and a different analytical strategy than that reported here would be required.

ACKNOWLEDGMENTS

Thanks are due to friends and colleagues who supplied material for this study. Technical assistance was received from Dr. S.J.B. Reed, electron microprobe; I.C. Marshall, SEM; A.R. Abraham, XRD; D. Symmons, photography. Assistance was received from Alan Smith and Lawrence Rush on use of the program ''TIME TREK-4'' for reconstructing paleolatitudinal position of the specimens. An earlier draft of this manuscript was improved by Stephanie De Villiers. Scott Carpenter, Tim Lowenstein, Arndt Peterhänsel, Associate Editor Bob Goldstein, and Editor David Budd are thanked for their terrific reviews that transformed the paper.

REFERENCES

Alexandersson, T., 1972, Intragranular growth of marine aragonite and Mg-calcite: evidence of precipitation from supersaturated seawater: Journal of Sedimentary Petrology, v. 47, p. 441–460.

Andrews, J.E., 1988, Methane-related Mg-calcite cements in recent tidal flat sediments from the Firth of Forth: Scottish Journal of Geology, v. 24, p. 233–244.

Ayora, C., Cendón, D.I., Taberner, C., and Pueyo, J.J., 2001, Brine–mineral reactions in evaporite basins: Implications for the composition of ancient oceans: Geology, v. 29, p. 251–254.

Bates, N.R., and Brand, U., 1990, Secular variation of calcium carbonate mineralogy; an evaluation of ooid and micrite chemistries: Geologische Rundschau, v. 79, p. 27–46.

Berner, R.A., 1978, Equilibrium, kinetics, and the precipitation of magnesian calcite from seawater: American Journal of Science, v. 278, p. 1435–1477.

Berner, R.A., Lasaga, A.C., and Garrels, R.M., 1983, The carbonate–silicate geochemical cycle and its effect on atmospheric carbon dioxide over the past 100 million years: American Journal of Science, v. 283, p. 641–683.

Brennan, S.T., and Lowenstein, T.K., 2002, The major-ion composition of Silurian seawater: Geochimica et Cosmochimica Acta v. 66, p. 2683–2700.

BUDD, D.A., 1992, Dissolution of high-Mg calcite fossils and the formation of biomolds during mineralogical stabilization: Carbonates and Evaporites, v. 7, p. 74–81.

BUDD, D.A., AND HIATT, E.E., 1993, Mineralogical stabilization of high-magnesium calcite: geochemical evidence for intracrystal recrystallization within Holocene porcellaneous foraminifera: Journal of Sedimentary Petrology, v. 63, p. 281–274.

BURNS, S.J., MCKENZIE, J.A., AND VASCONCELOS, C., 2000, Dolomite formation and biogeochemical cycles in the Phanerozoic: Sedimentology, v. 47, (Supplement 1), p. 49–61.

BURTON, E.A., 1993, Controls on marine carbonate cement mineralogy: review and reassessment: Chemical Geology, v. 105, p. 163–179.

BURTON, E.A., AND WALTER, L.M., 1991, The effects of P_{CO_2} and temperature on magnesium incorporation in calcite in seawater and $MgCl_2$–$CaCl_2$ solutions: Geochimica et Cosmochimica Acta, v. 55, p.777–785.

CARPENTER, S.J., AND LOHMANN, K.C., 1992, Sr/Mg ratios of modern marine calcite: empirical indicators of ocean chemistry and precipitation rate: Geochimica et Cosmochimica Acta, v. 56, p.1837–1849.

CARPENTER, S.J., LOHMANN, K.C., HOLDEN, P., WALTER, L.M., HUSTON, T.J., AND HALLIDAY, A.N., 1991, $\delta^{18}O$ values, $^{87}Sr/^{86}Sr$ and Sr/Mg ratios of Late Devonian abiotic marine calcite: Implications for the composition of ancient seawater: Geochimica et Cosmochimica Acta, v. 55. p. 1991–2010.

CHAVE, K., 1954, Aspects of the biogeochemistry of magnesium 1. Calcareous marine organisms: Journal of Geology, v. 62, p. 266–283.

CICERO, A.D., AND LOHMANN, K.C., 2001, Sr/Mg variation during rock–water interaction: Implications for secular changes in the elemental chemistry of ancient seawater: Geochimica et Cosmochimica Acta, v. 65, p. 741–761.

DAVIES, G.R., 1977, Former magnesian calcite and aragonite submarine cements in upper Paleozoic reefs of the Canadian Arctic: a summary: Geology, v. 5, p. 11–15.

DAVIES, K.J., DOVE, P.M., AND DE YOREO, J.J., 2000, The role of Mg^{2+} as an impurity in calcite growth: Science, v. 290, p. 1134–1137.

DICKSON, J.A.D., 1995, Paleozoic Mg calcite preserved: Implications for the Carboniferous ocean: Geology, v. 23, p. 535–538.

DICKSON, J.A.D., 2001a, Transformation of echinoid Mg calcite skeletons by heating: Geochimica et Cosmochimica Acta v. 65. p. 443–454.

DICKSON, J.A.D., 2001b, Diagenesis and crystal caskets: Echinoderm Mg calcite transformation, Dry Canyon, New Mexico, U.S.A: Journal of Sedimentary Research, v. 71, p. 764–777.

DICKSON, J.A.D., 2002, Echinoderm skeletal preservation: Calcite/aragonite seas and the Mg/Ca ratio of Phanerozoic oceans: Science, v. 298, p. 1222–1224.

DUBOIS, P., 1991, Morphological evidence of coherent organic material within the stereom of postmetamorphic echinoderms, *in* Suga, S., and Nakahara, H., eds., Mechanisms and Phylogeny of Mineralization in Biological Systems: New York, Springer-Verlag, p. 41–45.

ELDERFIELD, H., AND GANSSEN, G., 2000, Past temperatures and $\delta^{18}O$ of surface ocean waters inferred from foraminiferal Mg/Ca ratios: Nature, v. 405, p. 442–445.

FISHER, A.G., 1981, Climatic oscillations in the biosphere, *in* Nitecki, M., ed., Biotic Crises in Ecological and Evolutionary Time: New York, Academic Press, p. 103–131.

FRANK, T.D., AND LOHMANN, K.C., 1996, Diagenesis of fibrous magnesian calcite cement: Implications for the interpretation of $\delta^{18}O$ and $\delta^{13}C$ values of ancient equivalents: Geochimica et Cosmochimica Acta, v. 60, p. 2427–2436.

GAFFEY, S.J., KOLAK, J.J., AND BRONNIMANN, C.E., 1991, Effects of drying, heating, annealing, and roasting on carbonate skeletal material, with geochemical and diagenetic implications: Geochimica et Cosmochimica Acta, v. 55, p. 1627–1640.

GIVEN, R.K., AND WILKINSON, B.H., 1985, Kinetic control of morphology, composition, and mineralogy of abiotic sedimentary carbonates: Journal of Sedimentary Petrology, v. 55, p. 109–119.

GIVEN, R.K., AND WILKINSON, B.H., 1987, Dolomite abundance and stratigraphic age constraint on rates and mechanisms of Phanerozoic dolostone formation: Journal of Sedimentary Petrology, v. 57, p. 1068–1078.

GINSBURG, R.N., AND SCHROEDER, J.H., 1973, Growth and submarine fossilization of algal cup reefs, Bermuda: Sedimentology, v. 20, p. 575–614.

HARDIE, L.A., 1996, Secular variation in seawater chemistry: An explanation for the coupled secular variation in the mineralogies of marine limestones and potash evaporites over the past 600 my: Geology, v. 24, p. 279–283.

HARTLEY, G., AND MUCCI, A., 1996, The influence of P_{CO_2} on the partitioning of magnesium in calcite overgrowths precipitated from artificial seawater at 25° and 1 atm total pressure: Geochimica et Cosmochimica Acta, v. 60, p. 315–324.

HARVIE, C.E., MØLLER, N., AND WEARE, J.H., 1984, The prediction of mineral solubilities in natural waters: The Na–K–Mg–Ca–H–Cl–SO_4–OH–HCO_3–CO_3–CO_2–H_2O system to high ionic strengths at 25°C: Geochimica et Cosmochimica Acta, v, 48. p. 723–751.

HASTINGS, D.W., RUSSELL, A.D., AND EMERSON, S.R., 1998, Foraminiferal magnesium in *Globeriginoides sacculifer* as a paleotemperature proxy: Paleoceanography, v. 13, p. 161–169.

HOLLAND, H.D., 1978, The Chemistry of the Atmosphere and Oceans: New York, John Wiley, 351 p.

HOLLAND, H.D., AND ZIMMERMANN, H., 2000, The dolomite problem revisited: International Geology Review, v. 12, p. 481–490.

HOLLAND, H.D., HORITA, J., AND SEYFRIED, W.E., JR., 1996, On secular variations in the composition of Phanerozoic marine potash evaporites: Geology, v. 24, p. 993–996.

HORITA, J., ZIMMERMANN, H., AND HOLLAND, H.D., 2002, Chemical evolution of seawater during the Phanerozoic: Implications from the record of marine evaporites: Geochimica et Cosmochimica Acta, v. 66, p. 3733–3756.

JAMES, N.P., GINSBURG, R.N., MARSZALEK, D.S., AND CHOQUETTE, P.W., 1976, Facies and fabric specificity of early subsea cements in shallow Belize (British Honduras) reefs: Journal of Sedimentary Petrology, v. 46, p. 523–544.

KERR, R.A., 2002, Inconstant ancient seas and life's path: Science, v. 298, p. 1165–1166.

KOSTECKA, A., 1972, Calcite paramorphs in the aragonite concretions: Rocznik Polskiego towarzystwa geolgicznego, v. 42, p. 289–296.

KOVALEVICH, V.M., PERYT, T.M., AND PETRICHENKO, O.I., 1998, Secular variation in seawater chemistry during the Phanerozoic as indicated by brine inclusions in halite: Journal of Geology, v. 106, p. 695–712.

LAFON, G.M., AND VACHER, H.L., 1975, Diagenetic reactions as stochastic processes: application to the Bermudian eolianites, *in* Whitten, E.H.T., ed., Quantitative Studies in the Geological Sciences: Geological Society of America, Memoir 142, p. 187–204.

LAND, L.S., 1967, Diagenesis of skeletal carbonates: Journal of Sedimentary Petrology, v. 37, p. 914–930.

LASAGA, A.C., BERNER, R.A., AND GARRELS, R.M., 1985, An improved geochemical model of atmospheric CO_2 fluctuations over the past 100 million years, *in* Sundquist, E.T., and Broecker, W.S., eds., The Carbon Cycle and Atmospheric CO_2; Natural Variations Archean to Present: American Geophysical Union, Geophysical Monograph 32, p. 397–411.

LASEMI, Z., AND SANDBERG, P.A., 1984, Transformation of aragonite-dominated lime muds to microcrystalline limestones: Geology, v. 12, p. 420–423.

LEAR, C.H., ELDERFIELD, H., AND WILSON, P.A., 2000, Cenozoic deep-sea temperatures and global ice volumes from Mg/Ca in benthic foraminiferal calcite: Science, v. 287, p. 267–272.

LEMARCHAND, F., 2003, L'inconstance de l'eau de mer: La Recherche, no. 360, p. 14.

LOWENSTEIN, T.K., TIMOFEEFF, M.N., BRENNAN, S.T., HARDIE, L.A., AND DEMICCO, R.V., 2001, Oscillations in Phanerozoic seawater chemistry: evidence from fluid inclusions: Science, v. 294, p. 1086–1088.

LOHMANN, K.C., AND MEYERS, W.J., 1977, Microdolomite inclusions in cloudy prismatic calcites: a proposed criterion for former high magnesium calcites: Journal of Sedimentary Petrology, v. 47, p. 1078–1088.

MACKENZIE, F.T., AND PIGOTT, J.D., 1981, Tectonic controls of Phanerozoic sedimentary rock cycling: Geological Society of London, Journal, v. 138, p. 183–196.

MACKENZIE, F.T., BISCHOFF, W.B., BISHOP, F.C., LOIJENS, M., SCHOONMAKER, J., AND WOLLAST, R., 1983, Magnesian calcites: low-temperature occurrence, solubility and solid-solution behavoir, *in* Reeder, R.J., ed., Carbonates: Mineralogy and Chemistry: Mineralogical Society of America, Reviews in Mineralogy, v. 11, Chapter 4, p. 97–144.

MCKENZIE, J.A., AND BERNOULLI, D., 1982, Geochemical variations in Quaternary hardgrounds from the Helenic Trench region and possible relationship to their tectonic setting: Tectonophysics, v. 86. p. 149–157.

MACINTYRE, I.G., 1977, Distribution of submarine cements in a modern Caribbean fringing reef, Galeta Point, Panama: Journal of Sedimentary Petrology, v. 47, p. 503–516.

MEYERS, W.J., AND LOHMANN, K.C., 1978, Microdolomite-rich syntaxial cements: proposed meteoric–marine mixing zone phreatic cements from Mississippian limestones, New Mexico: Journal of Sedimentary Petrology, v. 48, p. 475–488.

MILLIMAN, J.D., AND MÜLLER, J., 1973, Precipitation and lithification of magnesian calcite in the deep-sea sediments of the eastern Mediterranean Sea: Sedimentology, v. 20, p. 29–45.

MONTAÑEZ, I.P., 2002, Biological skeletal carbonate records changes in major-ion chemistry of paleo-oceans: National Academy of Sciences, U.S.A., Proceedings, v. 99, p. 15,852–15,854.

MORSE, J.W., AND BENDER, M.L., 1990, Partition coefficients in calcite: Examination of factors influencing the validity of experimental results and their application to natural systems: Chemical Geology, v. 82, p. 265–277.

MORSE, J.W., AND MACKENZIE, F.T., 1990, Geochemistry of Sedimentary Carbonates: Amsterdam, Elsevier, Developments in Sedimentology 48, 707 p.

MORSE, J.W., WANG, Q., AND TSIO, M.Y., 1997, Influence of temperature and Mg:Ca ratio on $CaCO_3$ precipitates from seawater: Geology, v. 25, p. 85–87.

MUCCI, A., 1987, Influence of temperature on the composition of magnesian calcite overgrowths precipitated from seawater: Geochimica et Cosmochimica Acta, v. 51, p. 1977–1984.

MUCCI, A., AND MORSE, J.W., 1983, The incorporation of Mg^{2+} and Sr^{2+} into calcite overgrowths: influence of growth rate and solution composition: Geochimica et Cosmochimica Acta, v. 47, p. 217–233.

MÜLLER, J., AND FABRICIUS, F., 1974, Magnesian-calcite nodules in the Ionian deep sea: an actualistic model for the formation of some nodular limestones, *in* Hsü, K.J., and Jenkyns, H.C., eds., Pelagic Sediments: On Land and Under the Sea, International Association of Sedimentologists, Special Publication 1, p. 235–247.

NÜRNBERG, D., BUMA, J., AND HEMLEBEN, C., 1996a, Assessing the reliability of magnesium in foraminiferal calcite as a proxy for water mass temperatures: Geochimica et Cosmochimica Acta, v. 60, p. 803–814.

NÜRNBERG, D., BUMA, J., AND HEMLEBEN, C., 1996b, ERRATUM: Assessing the reliability of magnesium in foraminiferal calcite as a proxy for water mass temperatures: Geochimica et Cosmochimica Acta, v. 60, p. 2483–2484.

PATTERSON, W.P., AND WALTER, L.M., 1994, Syndepositional diagenesis of modern platform carbonates: Evidence from isotopic and minor element data: Geology, v. 22, p. 127–130.

PIGOTT, J.D., AND LAND, L.S., 1986, Interstitial water chemistry of Jamaican reef sediment: sulfate reduction and submarine cementation: Marine Geology, v. 19, p. 355–378.

PIRRIE, D., MARSHALL, J.D., AND CRAME, J.A., 1998, Marine high Mg calcite cements in *Teredolites*-bored fossil wood: evidence for cool paleoclimates in the Eocene La Meseta Formation, Seymour Island, Antarctica: Palaios, v. 13, p. 276–286.

REEDER, R.J., AND GRAMS, J.C., 1987, Sector zoning in calcite cement crystals: implications for trace element distribution in carbonates: Geochimica et Cosmochimica Acta, v. 51, p. 187–194.

RICHTER, D.K., 1974, Zur subaerischen Diagenese von Echinidenskeletten und das relative Alter pleistozäner Karbonatterrassen bei Korinth (Griechenland): Neues Jahrbuch für Geologie und Paläontologie, Abhandlungen, v. 146, p. 51–77.

RICHTER, D.K., 1984, Zur Zusammensetzung und Diagenese natürlicher Mg-calcite: Bochumer Geologische und Geotechnische Arbeiten, v. 15, 310 p.

RIMSTIDT, J.D., BALOG, A., AND WEBB, J., 1998, Distribution of trace elements between carbonate minerals and aqueous solutions: Geochimica et Cosmochimica Acta, v. 62, p. 1851–1863.
ROWLEY, D.B., 2002, Rate of plate creation and destruction: 180 Ma to present: Geological Society of America, Bulletin, v. 114, p. 927–933.
SANDBERG, P.A., 1975, New interpretations of Great Salt Lake ooids and of ancient nonskeletal carbonate mineralogy: Sedimentology, v. 22, p. 497–538.
SANDBERG, P.A., 1983, An oscillating trend in Phanerozoic nonskeletal carbonate mineralogy: Nature, v. 305, p. 19–22.
SAVARESE, M., DODD, J.R., AND LANE, N.G., 1996, Taphonomic and sedimentologic implications of crinoid intraskeletal porosity: Lethaia, v. 29, p. 141–156.
SCHERER, M., 1977, Preservation, alteration and multiple cementation of aragonite skeletons from the Cassian Beds (U. Triassic, southern Alps): Petrographic and geochemical evidence: Neues Jahrbuch für Geologie und Paläontologie, Abhandlungen, v. 154, p. 213–262.
SCHLAGER, W., AND JAMES, N.P., 1978, Low-magnesian calcite limestones forming at the deep-sea floor, Tongue of the Ocean, Bahamas: Sedimentology, v. 25, p. 675–702.
SMITH, A.B., 1980, Stereom microstructure of the echinoid test: Special Papers in Palaeontology, v. 25, p. 1–81.
SPENCER, R.J., AND HARDIE, L.A., 1990, Control of seawater composition by mixing of river waters and mid-ocean ridge hydrothermal brines, *in* Spencer, R.J., and Chou, I.-M., eds., Fluid–Mineral Interactions: A tribute to H.P. Eugter: The Geochemical Society, Special Publication 19, p. 409–419.
STANLEY, S.M., AND HARDIE, L.A., 1998, Secular oscillations in the carbonate mineralogy of reef-building and sediment-producing organisms driven by tectonically forced shifts in seawater chemistry: Palaeogeography, Palaeoclimatology, Palaeoecology, v. 144, p. 3–19.
STANLEY, S.M., AND HARDIE, L.A., 1999, Hypercalcification: Paleontology links plate tectonics and geochemistry to sedimentology: GSA Today, v. 9, no. 2, p. 1–7.
STANLEY, S.M., RIES, J.B., AND HARDIE, L.A., 2002, Low-magnesium calcite produced by coralline algae in seawater of Late Cretaceous composition: National Academy of Sciences, U.S.A., Proceedings, v. 99, p. 15,323–15,326.
TOBIN, K.J., AND WALKER, K.R., 1997, Ordovician oxygen isotopes and paleotemperatures: Palaeogeography, Palaeoclimatology, Palaeoecology, v. 129, p. 269–290.
WALKER, L.J., WILKINSON, B.H., AND IVANY, L.C., 2002, Continental drift and Phanerozoic carbonate accumulation in shallow-shelf and deep-marine settings: Journal of Geology, v. 110, p. 75–87.
WALLMANN, K., 2001, Controls on the Cretaceous and Cenozoic evolution of seawater composition, atmospheric CO_2 and climate: Geochimica et Cosmochimica Acta, v. 65, p. 3005–3025.
WEBER, J.N., 1969, The incorporation of magnesium into the skeletal calcites of echinoderms: American Journal of Science, v. 267, p. 537–566.
WEBER, J.N., 1973, Temperature dependence of magnesium in echinoid and asteroid skeletal calcite: a reinterpretation of its significance: Journal of Geology, v. 81, p. 543–556.
WHITTAKER, S.G., JAMES, N.P., AND KYSER, T.K., 1994, Geochemistry of synsedimentary cements in Early Cambrian reefs: Geochimica et Cosmochimica Acta, v. 58, p. 5567–5577.
WILKINSON, B.H., AND ALGEO, T.J., 1989, Sedimentary carbonate record of calcium–magnesium cycling: American Journal of Science, v. 289, p. 1158–1194.
WILKINSON, B.H., AND GIVEN, K.R., 1986, Secular variation in abiotic marine carbonates: Constraints on Phanerozoic atmospheric carbon dioxide contents and oceanic Mg/Ca ratios: Journal of Geology, v. 94, p. 321–333.
WILSON, P.A., AND DICKSON, J.A.D., 1996, Radiaxial calcite: Alteration product of and petrographic proxy for magnesian calcite cement: Geology, v. 24, p. 945–948.
WOO, K.-S., ANDERSON, T.F., AND SANDBERG, P.A., 1993, Diagenesis of skeletal and nonskeletal components of Mid-Cretaceous limestones: Journal of Sedimentary Petrology, v. 63, p. 18–32.
WOOD, A.D., BOTTJER, D.J., MUTTI, M., AND MORRISON, J., 1999, Lower Triassic large sea-floor carbonate cements: Their origin and a mechanism for the prolonged biotic recovery from the end-Permian mass extinction: Geology, v. 27, p. 645–648.
ZEEBE, R.E., AND SANYAL, A., 2002, Comparison of two potential strategies of planktonic foraminifera for house building: Mg^{2+} or H^+ removal? Geochimica et Cosmochimica Acta, v. 66, p. 1159–1169.
ZHANG, Y., AND DAWE, R.A., 2000, Influence of Mg^{2+} on the kinetics of calcite precipitation and calcite crystal morphology: Chemical Geology, v. 163, p. 129–138.
ZIMMERMANN, H., 2000, Tertiary seawater chemistry—implications from primary fluid inclusions in marine halite: American Journal of Science, v. 300, p. 723–767.
ZIMMERMANN, H., 2001, On the origin of fluids included in Phanerozoic marine halite—basic interpretation strategies: Geochimica et Cosmochimica Acta, v. 65, p. 35–45.

Received 16 April 2003; accepted 22 November 2003.